

TWO NEW EXTREMELY IRON-RICH HOT DA WHITE DWARFS AND THE NATURE OF THE EUV OPACITY

J. B. HOLBERG,^{1,2} M. A. BARSTOW,^{3,4} D. A. H. BUCKLEY,⁵ A. CHEN,⁶ S. DREIZLER,⁷ M. C. MARSH,⁴
D. O'DONOGHUE,⁶ E. M. SION,⁸ R. W. TWEEDY,⁹ G. VAUCLAIR,¹⁰ AND K. WERNER^{7,11}

Received 1993 February 19; accepted 1993 April 27

ABSTRACT

We have obtained *IUE* echelle spectra of two bright extreme ultraviolet (EUV) sources discovered by the *ROSAT* wide field camera all-sky survey. These stars, RE 2214–492 and RE 0623–377, are previously uncataloged hot DA white dwarfs with respective apparent visual magnitudes of 11.71 and 12.09 and exhibit short-wavelength EUV cutoffs steeper than most other DAs. The *IUE* echelle spectra are rich in absorption lines due to a large number of Fe v and Fe vi features, in addition to the highly ionized C, N, O ions frequently seen in other hot DA white dwarfs. No He is observed in either star. Comparison of RE 2214–492 and RE 0623–377 with two well-studied hot DA white dwarfs, G191 B2B and Feige 24, indicates that these new stars are both significantly hotter and more metal-rich than G191 B2B and Feige 24. From optical and UV line profiles we find $T_{\text{eff}} = 63,500$ K and 60,300 K for RE 2214–492 and RE 0623–377, respectively. From modeling of Fe v features in the echelle spectra we find corresponding Fe abundances of $\log [N(\text{Fe})/n(\text{H})] = -4.25 \pm 0.25$. The association of steep EUV cutoffs in these stars, and in G191 B2B and Feige 24, with the observed presence of Fe suggests that iron-group elements along with other heavy elements are responsible for much of the EUV opacity observed by *ROSAT* in the hottest DA stars.

Subject headings: star: individual (RE 2214–492, RE 0623–377) — white dwarfs — stars: abundances — ultraviolet: stars

1. INTRODUCTION

The beginning of systematic observations in the Extreme Ultraviolet (EUV) band, first by *ROSAT* in 1990 and recently by the *Extreme Ultraviolet Explorer (EUVE)* launched in 1992, has renewed interest in the origin of the short-wavelength opacity observed in white dwarfs. Since the initial analysis of *Einstein* soft X-ray data from a small sample of white dwarfs by Kahn et al. (1984), it has been apparent that the fluxes of many ostensibly pure H (DA) white dwarfs have soft X-ray and EUV fluxes which are significantly lower than predicted. The early attempts to model this effect assumed that the extra opacity is provided by He, and much work has been published (e.g., Petre, Shipman, & Canizares 1986; Jordan et al. 1987; Paerels & Heise 1989; Koester 1989) using EUV data to derive He abundances. At the time *ROSAT* began its all-sky survey it was still believed that this prescription largely remained valid, although there were some contradictory indications. Two basic photospheric structures were considered. One envisaged that

the H and He were homogeneously mixed, with the He content being maintained by radiation pressure. However, Vennes et al. (1988) have shown that this mechanism cannot support He in a white dwarf gravitation field, and that a homogeneously mixed photosphere would rapidly reach an equilibrium configuration in which the H and He were separated. Such a stratified structure represents the second idea discussed in the literature. It is a necessary aspect of such a model that the H layer be ultrathin, otherwise the He opacity, which is masked at optical and UV wavelengths, would also be obscured in the EUV. However, there has been no convincing observational evidence, in any wavelength region, that the He inferred in DA white dwarfs from the soft X-ray and EUV observations is actually present in the photospheres of these stars at anywhere near the required levels. While He may exist at trace levels in some DA photospheres, and is clearly evident in DAO and DAB white dwarfs, there is as yet no spectroscopic link between this He and the short-wavelength opacity.

The *ROSAT* wide field camera (WFC) has provided the first global insight into EUV flux distributions for a large sample of DA white dwarfs. It conducted the first all-sky EUV survey in two bands, the 60–140 Å S1 band and the 112–200 Å S2 band. The subsequent catalog of EUV sources (Pounds et al. 1993) contains 119 identified hot white dwarfs. Barstow et al. (1993) considered *ROSAT* observations of some 30 of these hot DA white dwarfs for which reliable temperatures and gravities were also available from optical and ultraviolet observations. The EUV fluxes from the two WFC survey bands and the soft X-ray fluxes from the position-sensitive proportional counter (PSPC) were used to test the predictions of DA model atmospheres containing both homogeneously mixed H+He and stratified H+He atmospheres. For stars below $\sim 40,000$ K, trace amounts of He are consistent with the *ROSAT* data. However, nearly all stars above this temperature exhibit steeper EUV cutoffs than can be explained by H+He opacity

¹ Guest Observer, *International Ultraviolet Explorer* satellite.

² Lunar and Planetary Laboratory, University of Arizona, Gould Simpson Bld., Tucson, AZ 85721.

³ Guest Observer, *Voyager* ultraviolet spectrometers.

⁴ X-Ray Astronomy Group, University of Leicester, Leicester, LE1 7RH, UK.

⁵ South African Astronomical Observatory, Cape Town, South Africa.

⁶ Dept. Astronomy, University of Cape Town, Rondebosch 7700, South Africa.

⁷ Dr.-Remeis-Sternwarte, Universität Erlangen-Nürnberg, Sternwartweg 7, W-8600 Bamberg, FRG.

⁸ Department of Astronomy and Astrophysics, Villanova University, Villanova, PA 19085.

⁹ Steward Observatory, University of Arizona, Tucson AZ 85721.

¹⁰ University Paul Sabatier, Observatoire Midi-Pyrenees, CNRS-URA, 285, F-3140, Toulouse, France.

¹¹ Institut für Theoretische Physik und Sternwarte, Universität Kiel, W23100 Kiel, FRG.

alone. In particular, neither stratified nor homogeneous H+He atmospheres were allowed by the *ROSAT* observations.

There are two current scenarios for the source of the soft X-ray and EUV opacity in DA white dwarfs, both of which have strong observational support and neither involves the presence of He. One dramatic observation is the unique EUV rocket spectrum of G191 B2B (Wilkinson, Green, & Cash 1992), which covers the 220–330 Å region. Their result, which showed no evidence of an He II 228 Å edge, revealed three strong edges which result in a factor of 5 decrease in flux from 260 Å to 220 Å. The authors suggest these edges are due to O III. A non-NLTE spectrum calculated by Napiwotzki, discussed in Tweedy (1993), shows that O IV and O V are the dominant oxygen ions expected in the photosphere of G191 B2B ($T_{\text{eff}} = 58,000$ K), and that little O III should be present. In principle, the O abundance could be increased until O III edges match those observed, but the weak UV lines of O IV and O V reported by Sion et al. (1992) and Tweedy (1991) place severe constraints on any self-consistent photospheric models. Thus, a circumstellar origin is suggested for some or most of the O III, perhaps due to a wind-ISM interaction as has been suggested in the case of GD 659 (MacDonald 1992). Limited EUV spectral results also exist for Feige 24. A low-resolution *EXOSAT* transmission grating spectrum (Paerels et al. 1986) showed a virtually featureless continuum steeply cut off at the shortest wavelengths. Paerels et al. were unable to explain the Feige 24 spectrum in terms of He, but Vennes et al. (1989) were able to do so using a photosphere containing a host of trace metals. Therefore, in the two existing cases of DA stars with strong short-wavelength opacities for which EUV spectral information exists, G191 B2B and Feige 24, their spectra have been interpreted in terms of elements other than He. This is in contrast to the considerable number of other hot DA white dwarfs whose observed soft X-ray/EUV fluxes have, until recently, been interpreted almost exclusively in terms of a photospheric He content.

Observationally, the presence of C, N, O, and Si in some hot DA white dwarfs has been evident since they were detected by Bruhweiler & Kondo (1981, 1983) in *IUE* echelle spectra. Recently, Fe has also been detected in the far-UV spectra of G191 B2B and Feige 24 by several observers. Sion et al. (1992) in the *Hubble Space Telescope* (*HST*) FOS spectrum of G191 B2B found eight individual features and 13 blended features corresponding to Fe V; in two instances these blends possibly contain lines due to Fe VI. In an analysis of co-added *IUE* spectra of G191 B2B, Tweedy (1991) identified up to 23 Fe V lines at equivalent widths of between 15 mÅ and 40 mÅ. He found no lines due to Fe VI. Vennes et al. (1992) also used co-added *IUE* echelle spectra to determine an Fe abundance of $\log [N(\text{Fe})/N(\text{H})] = -5.3$ for G191 B2B. Bruhweiler & Feibelman (1993) also report Fe in G191 B2B. Similar detections of Fe are reported for Feige 24 by Vennes et al. (1992) and Bruhweiler & Feibelman (1993). Both Sion et al. (1992) and Tweedy (1991) have pointed out that the observed Fe V transitions lie 23 eV above the ground state and must therefore be of photospheric origin.

While radiative levitation alone is unable to account for the postulated He abundances, this is not the situation for selected heavier elements. Several investigators have calculated the expected equilibrium abundances of C, N, O, and Si as a function of effective temperature and gravity in DA photospheres (Vauclair 1989; Chayer, Fontaine, & Wesemael 1989), and

these calculations have recently been extended to Fe by Chayer, Fontaine, & Wesemael (1991) and Vennes et al. (1992). They find that detectable amounts of Fe can be radiatively levitated in the photospheres of a $0.6 M_{\odot}$ DA white dwarf at temperatures above 50,000 K. Thus, on theoretical and observational grounds, it is extremely likely that Fe and other heavy elements contribute substantially to the EUV opacity of many hot DA white dwarfs.

A crude but effective measure of EUV opacity in DA stars can be obtained by examining their WFC S2:S1 count rate ratios. Barstow et al. (1993) have shown that hot white dwarfs having little or no EUV opacity and a low line-of-sight interstellar absorption, like HZ 43, have S2:S1 ratios of ~ 3 –4, while strongly opaque sources, such as G191 B2B and Feige 24, exhibit very large S2:S1 ratios of 42 and 144, respectively. Thus, DA stars with very large S2:S1 ratios are good candidates in which to seek spectroscopic evidence of trace elements which may be contributing to the EUV opacity. Among the DA white dwarfs in the WFC catalog some of the highest observed S2:S1 ratios belong to RE 2214–492 and RE 0623–377. Since these stars were detected only in the S2 band we are only able to quote lower limits to the ratio of greater than 69 and greater than 67, respectively. The extreme spectral slope is also evident from the fact that neither star was detected by the PSPC.

We report here the first optical and *IUE* observations of RE 2214–49 and RE 0623–37, concentrating in particular on the *IUE* echelle spectra. We outline the stellar and interstellar features present in these data, and note similarities between these two objects. We also compare RE 2214–492 and RE 0623–377 with G191 B2B and Feige 24 and discuss the interpretation of our results in terms of the early evolutionary phases of DA white dwarfs.

2. TEMPERATURE AND GRAVITY DETERMINATION FROM OPTICAL AND *IUE* DATA

RE 2214–492 and RE 0623–377 were first discovered through their detection by the *ROSAT* WFC and were first identified as DA white dwarfs during the subsequent program of optical spectroscopy to search those fields, where no cataloged object could be associated with the EUV source, for a plausible optical counterpart (Mason et al. 1993). The spectra indicated that both stars were very bright and very hot DA white dwarfs.

We have recently obtained the following $UBVR_c I_c$ magnitudes and colors for these two stars. The results, in addition to indicating that both stars are very blue, also demonstrate that both stars rank with G191 B2B ($V = 11.78$) as among the brightest of the hot DA white dwarfs (see Table 1). The “RE” designations for these stars derives from the observed J2000 coordinates of the WFC survey positions. We have measured the locations of these stars on the ESO Southern Survey plates and compared the results with the positions from the *HST* Guide Star Catalog (GSC). We find no significant difference between the positions at the respective epochs of 1976 and

TABLE 1
 $UBVR_c I_c$ DATA FOR PROGRAM

Star	V	$U-B$	$B-V$	$V-R$	$V-I$
RE 2214–492....	11.77	–1.22	–0.34	–0.18	–0.42
RE 0623–377....	12.09	–1.22	–0.33	–0.15	–0.05

1983. The mean ESO–GSC positions for both stars are as follows:

$$\text{RE 2214–492: } \alpha_{1950} 22^{\text{h}}11^{\text{m}}02^{\text{s}}.915 \delta_{1950} -49^{\circ}34'20''.030$$

$$\text{RE 0623–377: } \alpha_{1950} 06^{\text{h}}21^{\text{m}}30^{\text{s}}.130 \delta_{1950} -37^{\circ}39'51''.135.$$

A standard way to determine the temperature and gravity of DA white dwarfs is to fit synthetic line profiles to the observed Balmer and, where available, Lyman α line profiles (e.g., Kidder 1991 and Holberg et al. 1985). The original identification spectra were of too coarse a resolution and too low a signal-to-noise ratio (S/N) for this work. Consequently, new spectra were obtained using the 1.9 m reflector of the South African Astronomical Observatory (SAAO), equipped with an intensified Reticon spectrograph. A complete log of all observations of RE 2214–492 and RE 0623–377 is given in Table 2. The spectra covered the wavelength range 3600–5000 Å with a reciprocal dispersion of 75 Å mm⁻¹, yielding a resolution of ~2.5 Å. Flat-field spectra were obtained at the start and end of each night, and wavelength calibration was provided by a CuAr lamp which was observed at least every 20 minutes. Observations of spectrophotometric standard stars enabled the observed counts to be converted to flux units in the usual way. The Reticon data are sampled at 1 Å intervals but were then summed into 4 Å bins, to improve the S/N in the spectrum, before performing the spectral fitting. We find that, in both spectra, the H β , γ , and δ lines have good enough S/N to include in the spectral fitting but the higher lines in the series (H ϵ , etc.) are too weak to be useful. A turnover in the continuum of the RE 0623–377 spectrum at long wavelengths makes the H β line difficult to use. This is caused by temporal changes in instrument sensitivity between the observation of the flux standard and that of RE 0623–377. To avoid unquantifiable effects on the spectral fitting, we have chosen to use H γ and H δ only for this star. No features, other than H I Balmer lines, are evident in these spectra.

Low-resolution IUE SWP spectra, using both large and small apertures, were obtained for each star (see Table 2). In principal, small-aperture exposures exhibit less geocoronal Lyman- α contamination, allowing the intrinsic stellar Lyman- α profile to be fitted. Small-aperture spectra, which suffer from light loss, can be normalized to the large-aperture fluxes and

co-added with the large-aperture data. Lyman- α profiles obtained in a manner similar are described in Holberg, Wesemael, & Basile (1986) and Kidder (1991). For RE 2214–492 the stellar Lyman- α profile exhibited no detectable contamination for the geocoronal component. Unfortunately, the small-aperture spectrum of RE 0623–377 is sufficiently contaminated by geocoronal radiation that the Lyman- α profile was not useful for spectral fitting.

The synthetic line profiles were taken from an extensive grid of stratified H+He models calculated using the LTE code of Koester (see, e.g., Jordan & Koester 1986; Koester 1991). These models include full H and He line blanketing and span the temperature range from 20,000 to 100,000 K and cover 6.5–8.5 in log g . The thickness of the hydrogen layer mass runs from approximately 10⁻¹⁶ to 10⁻¹² M $_{\odot}$. At 10⁻¹² M $_{\odot}$ the layer mass is sufficiently large for the He opacity to be negligible, i.e., the atmosphere would appear to be pure hydrogen from the point of view of any observations. Although we believe, from the EUV data, that these stars contain trace heavy elements we do not expect their presence to affect the atmospheric structure in the regions where the Balmer and Lyman lines are formed (Dreizler & Werner 1993) and so the Koester H+He models can reasonably be used to determine the effective temperature and surface gravity for these stars.

The line profile fitting was performed with the X-ray spectral fitting package XSPEC (Shafer et al. 1991), extended to allow optical and IUE spectra to be treated using standard interfaces for user-supplied models and data. Best-fit models are found by the standard technique of searching for the set of model parameters that minimize a χ^2 statistic representing the difference between the model predictions and the data, taking into account the uncertainties in the observed fluxes. All the lines available for each star—H β , γ , δ , and Lyman- α for RE 2214–492; H γ and δ for RE 0623–377—were fitted simultaneously to the models with temperature, gravity, and layer mass all being allowed to vary independently. The best fits are shown in Figures 1 and 2, while the parameter values and the 1 σ error ranges are summarized in Table 3.

It is apparent that RE 2214–492 and RE 0623–377 are somewhat hotter than either G191 B2B or Feige 24 but, within the errors, have similar surface gravity. The H layer masses

TABLE 2
LOG OF OBSERVATIONS

Instrument IUE Image Number	Date	Exposure	Dispersion	Aperture
RE 2214–492				
SWP 44765	1992 May 25	162 s	Low	Large
SWP 44765	1992 May 25	324 s	Low	Small
SWP 44766	1992 May 25	2 hr	High	Large
SWP 44767	1992 May 25	2 hr	High	Large
SAAO 1.9 m	1992 Nov 22	400 s		
ROSAT	1990 Oct 11–Nov 4	(survey)		
ROSAT	1992 Nov 15/16	3775 s (pointed phase)		
RE 0623–377				
SWP 45950	1992 Oct 15	258 s	Low	Large
SWP 45951	1992 Oct 15	4 hr	High	Large
SWP 46303	1992 Nov 20	520 s	Low	Small
Voyager 1	1992 Jul 30–Aug 3	10.6 hr		
SAAO 1.9 m	1992 Nov 18	600 s		
ROSAT	1992 Aug 23–Oct 2	(survey)		
ROSAT	1992 Oct 20	(pointed phase)		

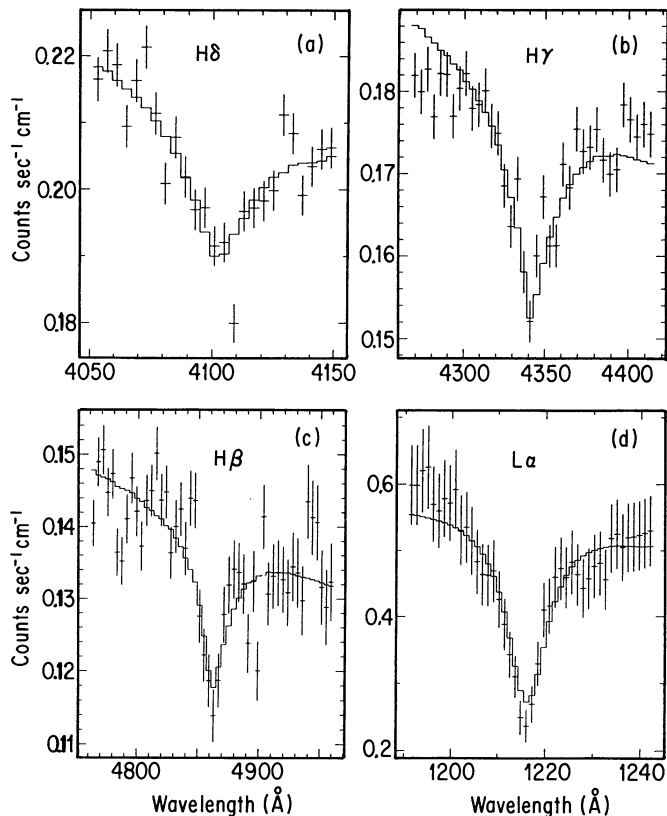


FIG. 1.—Model fits (histogram) to the observed Balmer and Lyman- α profiles (+) of RE 2214–492. The best-fitting model is defined by the parameters listed in Table 3. The uncertainties for individual data points are indicated by the vertical error bars.

contained in Table 3 result from our formal fitting procedure in which the H layer masses of our stratified models is a free parameter. In general, the influence of H layer masses in line profiles are not large—consequently this parameter is not well constrained as is clear from the range of the resulting uncertainties. Indeed, if we consider a more conservative limit of 95% confidence in the H layer mass determination, we find that an infinitely thick H layer mass is allowed. The lack of He II features allows us to place an independent constraint on allowable H layer mass. If the layer mass for either star were less than $10^{-14} M_{\odot}$, then He II features would become evident. It is reassuring that our layer masses are at least 1σ above this value.

3. IUE ECHELLE OBSERVATIONS

We have also obtained IUE echelle spectra of RE 2214–492 and RE 0623–377 as listed in Table 2. All three of the echelle

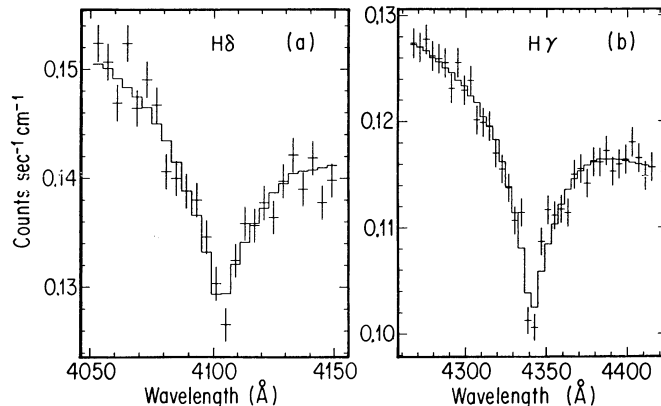


FIG. 2.—Same as for Fig. 1 but for the H δ and H γ profiles of RE 0623–377

spectra were fully exposed, although the RE 2214–492 (SWP 44766 and SWP 44767) spectra have superior S/N to that of RE 0623–377 (SWP 45951). The two RE 2214–492 echelle spectra were compared and found to be very nearly identical with respect to the features present and the wavelength scales. A careful determination of the apparent velocities associated with the strong C IV, N V, and Si IV doublets in both spectra revealed a small relative velocity shift of $+0.9 \pm 0.3 \text{ km s}^{-1}$ between the two echelle spectra. This differential velocity was therefore used to shift the wavelength scale of SWP 44767 to that of SWP 44766, prior to the co-addition of the two spectra. Standard IUE data processing and analysis software was used to produce all of the results presented here. All measured velocities are with respect to the heliocentric frame and the echelle wavelength scale obtained with standard IUE image processing. To facilitate identification of the numerous unmeasured weak features, however, the spectra were Doppler-shifted to the laboratory frame.

In Table 4 we present measurements of the velocities and equivalent widths of some of the stronger and more interesting features found in these spectra. These include a well-defined set of low-ionization features which we attribute to line-of-sight interstellar absorption, a large number of highly ionized features due to Fe V and Fe VI, and features due to high-ionization states of C, N, O, Si, and Al. Many of the highly ionized lines have been previously reported in other hot DA white dwarfs and hot degenerate objects. In our spectra they share a common radial velocity which is distinct from that of the interstellar features. Thus we attribute the highly ionized lines to the white dwarf photospheres. In addition to the features which can be identified with the above ions, we find that both spectra exhibit many additional features which may well be real, but cannot be consistently identified with any species. Below, we discuss each of these groups of features in turn.

TABLE 3
TEMPERATURE, GRAVITY, AND H LAYER MASS DETERMINATION

Parameter	Value	RE 2214–492 $\pm 1 \sigma$ range	Value	RE 0623–377 $\pm 1 \sigma$ range
$T_{\text{eff}}(\text{K})$	63,500	+1400 – 1400	60,300	+1700 – 1300
$\log g$	7.5	+0.04 – 0.08	7.34	+0.10 – 0.13
H mass (M_{\odot})	2.5×10^{-14}	$3\text{--}1.6 \times 10^{-14}$	2.5×10^{-14}	$4.6\text{--}1.4 \times 10^{-14}$

TABLE 4
MEASURED SPECTRAL FEATURES

ION	WAVELENGTH (Å)	RE 2214–492		RE 0623–377	
		V (km s ⁻¹)	E.W. (mÅ)	V (km s ⁻¹)	E.W. (mÅ)
Stellar Features					
N v	{ 1238.821	+35.7	163.3	+18.2	120.3
	{ 1242.804	+39.0	132.3	+19.3	112.4
N iv	{ 1718.551	+43.9	70.2	+15.9	54.2
	{ 1338.612	+43.9	49.4	+33.7	53.1
O iv	{ 1343.512	+46.3	47.6	+27.4	62.2
	{ 1371.292	+37.3	49.0	+15.4	40.2
O v	{ 1393.755	+38.8	94.1	+23.2	88.0
	{ 1402.770	+37.1	72.1	+24.4	87.0
C iv	{ 1548.202	+35.9	147.5	+22.8	111.3
	{ 1550.774	+39.9	149.1	+22.5	122.2
Al iii	{ 1854.716	+38.1	25.7	+22.7	51.1
	{ 1402.388	+39.5	27.5	+22.5	69.4
Fe v	{ 1430.573	+34.1	51.2	+21.7	30.9
	{ 1440.528	+35.6	16.3	+23.2	26.9
	{ 1448.846	+38.6	19.2	+27.9	41.8
	{ 1456.161	+55.7	50.7	+26.8	53.6
	{ 1469.000	+35.2	74.4	+20.1	37.9
	{ 1479.471	+32.7	42.4	+13.1	42.2
	{ 1252.782	+45.7	35.0		
Fe vi	{ 1272.065	+36.0	31.0		
	{ 1276.876	+47.2	58.1	+29.8	49.5
	{ 1294.546	+19.9	26.5
Weighted average		+38.9 ± 6.7 km s ⁻¹		+22.5 ± 5.0 km s ⁻¹	
Interstellar Features					
N i	{ 1199.5490	-1.7	71.5	-0.1	99.5
	{ 1200.2238	+3.8	58.4	+1.7	53.2
	{ 1200.7113	+6.1	44.0	+2.2	68.2
Si ii	{ 1190.4157	+11.6	110.3	-2.8	71.1
	{ 1193.2894	+10.2	105.9	+7.1	64.2
	{ 1260.4212	+7.8	143.1	-1.2	97.2
	{ 1526.7076	+7.0	83.7	+4.2	68.1
Si iii	{ 1206.510				
	{ 1206.533	+9.1	120.1		
C ii	1334.5323	+2.4	155.1	+0.3	113.8
Weighted average		+6.6 ± 3.9 km s ⁻¹		+1.1 ± 2.9 km s ⁻¹	

3.1. Interstellar Features

Low-ionization features of interstellar origin are present in both spectra; these include N i, Si ii, and C ii. In Table 3 we provide the measured radial velocities and strengths for these lines. In both stars we find consistent velocities for these interstellar features which are distinct from the velocities of the higher ionization state lines. We obtain average velocities of $+6.6 \pm 3.9$ km s⁻¹ and $+1.1 \pm 2.9$ km s⁻¹ for the interstellar medium (ISM) features in RE 2214–492 and RE 0623–377, respectively. The only notable difference between RE 2214–492 and RE 0623–377 with respect to these interstellar features is the lack of a measurable Si iii λ 1206 feature in RE 0623–377. The velocities of these interstellar features differ somewhat from predicted velocities based on determinations of the relative velocity vector between the local ISM and the solar system. For example, the Crutcher (1982) vector predicts -9.1 km s⁻¹ and $+21.3$ km s⁻¹ for the velocities of the ISM features in RE 2214–492 and RE 0623–377, respectively, while the recent velocity vector of Lallement et al. (1992) predicts respective velocities of -8.6 and $+14.1$ km s⁻¹. However, given the uncertainties associated with the local ISM velocity vectors, the precise placement of the stars within the SWP large aperture and the apparent secular trend in measured

SWP radial velocities (Mansperger 1992), such disagreements are not surprising.

3.2. Fe v and Fe vi

A large number of features due to Fe v are present in RE 2214–492 and RE 0623–377. Using the wavelengths and relative intensities of Ekberg (1975b) we have identified up to 66 features due to Fe v in RE 2214–492 and 45 features in RE 0623–377 over the wavelength range 1230–1570 Å. For RE 2214–492, this would include virtually all of the features between 1300 to 1500 Å with a relative intensity of “200” or greater in the line list of Ekberg (1975b). These identifications were obtained by Doppler-shifting the wavelength scale of each spectrum to the laboratory frame using the photospheric radial velocity previously determined for each star. The spectra were then displayed and the wavelengths of features which appeared to be lines were measured. Only after all features were measured were the resulting wavelengths compared with various published line lists, including Ekberg (1975a, b). Any feature differing by more than 0.01 Å was rejected as a possible match. In Figures 3 and 4 we show the respective 1370–1381 Å and 1440–1456 Å regions of both spectra where numerous Fe v features are evident. In Table 4 we provide measured

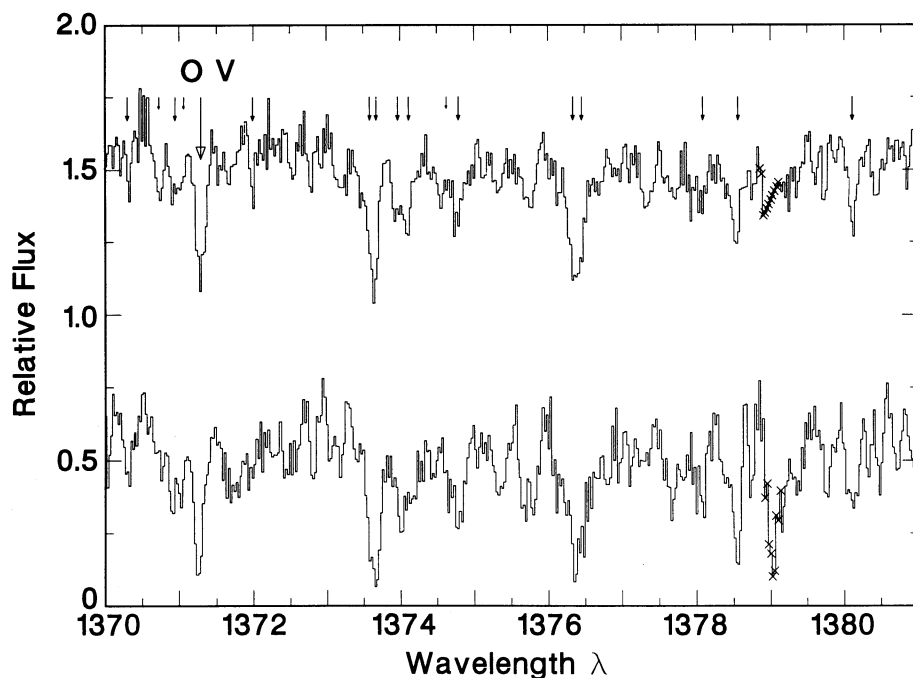


FIG. 3.—The 1370–1381 Å regions of RE 2214–492 (*top*) and RE 0623–377 (*bottom*). The long arrows indicate the locations of Fe v lines having relative intensities greater than “200” in Ekberg (1975a), while the short arrows correspond to Fe vi lines having relative intensities of greater than “300” or greater from Ekberg (1975b). The fluxes for RE 2214–492 and RE 0623–377 have been offset by +0.5 and –0.5, respectively. Wavelength scales for both stars have been Doppler-shifted to the laboratory frame.

velocities and equivalent widths for seven of the stronger Fe v features present in both spectra. It is clear from the line list of Ekberg (1975b) and our examination of both spectra that even more Fe v lines should be evident in higher S/N data.

We also find good evidence for up to 17 features due to Fe vi in RE 2214–492. With the exception of Fe vi 1276.96 Å, no feature due to this ion can be confidently identified in RE 0623–377. Again, this may simply be due to the combined

effects of the lower overall S/N and the lower observed Fe vi equivalent widths in the RE 0623–377 spectrum. In Figure 5 we show the 1271–1282 Å region of both stars together with the locations of Fe vi lines occurring in this wavelength range. We have plotted all Fe vi lines with relative intensities greater than “300” from the study of Ekberg (1975a). In Table 4 we also list the observed velocities of the four strongest Fe vi features found in RE 2214–492. It should be noted that while

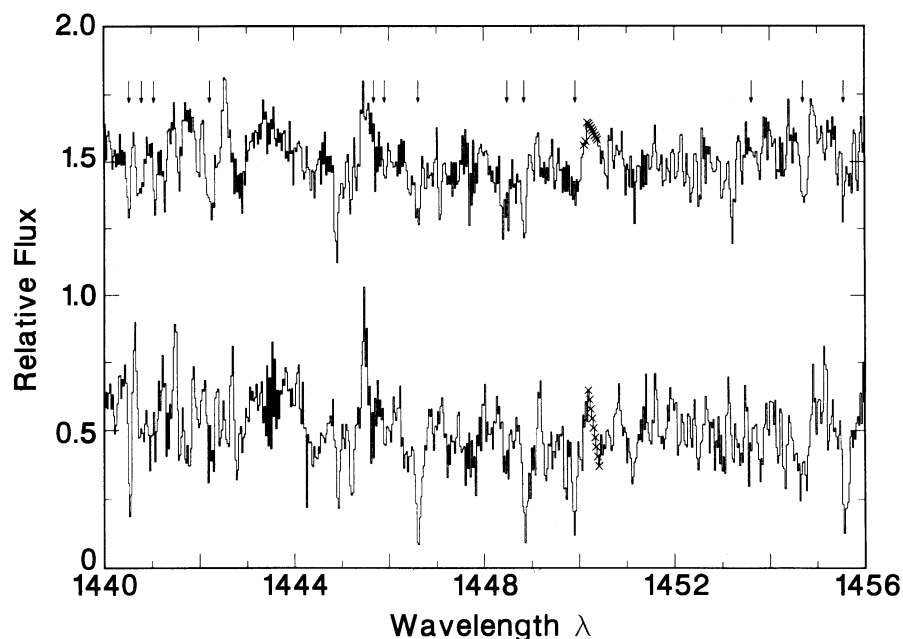


FIG. 4.—The same as Fig. 3, but showing the 1440–1456 Å region

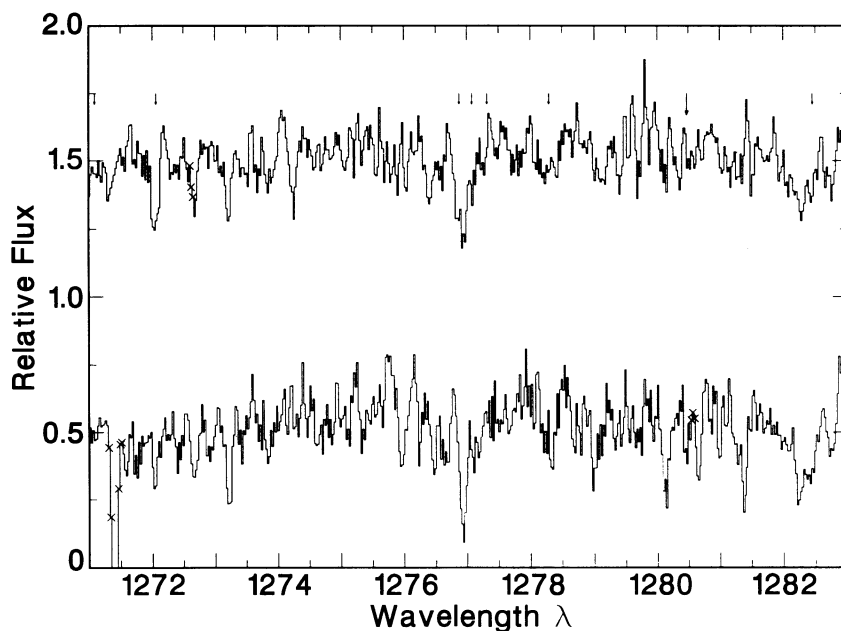


FIG. 5.—The same as Fig. 1, but showing the 1271–1283 Å region containing several Fe VI lines

Fe VI has been reported in the *IUE* echelle spectra of hot subdwarfs and the central stars of planetary nebulae (PNs) (Dean & Bruhweiler 1985; Feibelman & Bruhweiler 1989; Tweedy & Napiwotzki 1992), it has not previously been detected in any DA white dwarf. Possible blends of features involving Fe VI lines are noted in the FOS G191 B2B spectrum by Sion et al. (1992) but the spectral resolution is not sufficient to resolve them. As yet no Fe VI lines have been found in co-added *IUE* echelle spectra of G191 B2B (Tweedy 1991).

It is the presence of these Fe V and Fe VI lines that provides the strongest argument for a photospheric origin of the high-ionization features seen in RE 2214–492 and RE 0623–377. The Fe V features seen at *IUE* wavelengths arise from transitions between the $3d^34s$ and $3d^34p$ configurations and, as pointed out by Tweedy (1991) and Sion et al. (1992), the lower lying $3d^34s$ configuration is ~ 27 eV above the ground state. Likewise, the Fe VI transitions which we see arise from the $3d^24s$ configuration which is ~ 32 eV above the ground state. Such excited levels are never seen in the general ISM and have been reported only in the most extreme circumstellar environments such as the dense winds of Wolf-Rayet stars (Koenigsberger 1990). Our spectra show no evidence whatsoever of features associated with winds, dense or otherwise. In particular, there are no P Cygni profiles. Thus, we conclude that the Fe features and the other high-ionization state ions, which share a common radial velocity (see below), are photospheric in origin.

It is interesting to compare the average strengths of the Fe V lines in our two stars. From the measured equivalent widths of the seven Fe V lines in Table 4 we find a mean strength of 40.3 mÅ for RE 2214–492 and 46.2 mÅ in RE 0623–377. Thus, both stars appear to exhibit Fe V lines of similar strength and the greater number of lines found in RE 2214–492 is primarily a consequence of the greater S/N of its spectrum.

3.3. C, N, O, Si, and Al

The well-known doublets due to C IV, N V, and Si IV are prominent in both our spectra, as are lines due to N IV, O IV,

O V, and Al III. Observed radial velocities and equivalent widths are presented in Table 4. In Figure 6 we display the region containing the Si IV doublet in both spectra. To within measurement uncertainties, the strengths of most of these features are comparable in both RE 2214–492 and RE 0623–377. Most have previously been reported in one or more hot DA white dwarfs, except for N IV at 1718.555 Å and Al III at 1854.716 Å lines which have not been previously reported in a DA white dwarf. The identification of Al III is further strengthened by weak features at the locations of Al III $\lambda 1862.790$ in RE 0623–377 and Al III $\lambda 1379.67$ in RE 2214–492.

It is significant that for each star the measured velocities for all of these lines are consistent. In other degenerate stars (Sion & Downes 1992; Sion et al. 1992; and Vennes, Thejll, & Shipman 1991) where velocity differentials between species have been observed, this has been cited as evidence for the existence of winds and/or circumstellar matter. Taking the equivalent width-weighted averages of those due to C, N, O, Si, and Al we obtain $+38.8 \pm 3.3$ km s $^{-1}$ and $+22.5 \pm 5.0$ km s $^{-1}$ for RE 2214–492 and RE 0623–377, respectively. These values are also consistent with the averages independently determined for Fe V and Fe VI (RE 2214–492, $+39.3 \pm 8.8$ km s $^{-1}$, and RE 0623–377, $+23.4 \pm 4.9$ km s $^{-1}$). Combining all high-excitation features from Table 3, we derive weighted mean photosphere radial velocities of $+38.9 \pm 6.7$ km s $^{-1}$ for RE 2214–492 and $+22.5 \pm 5.0$ km s $^{-1}$ for RE 0623–377. Thus there appears to be no evidence in either star for significant velocity differentials between different species. This conclusion is significant since for both G191 B2B and Feige 24 there is evidence that at least some of these features arise from circumstellar material. In G191 B2B (Tweedy 1991) there are small apparent velocity differentials among some species. In Feige 24 there exist two distinct velocity systems for C IV, N V and Si IV; one associated with the orbital motion of the DA component and the other associated with gas in the system (Dupree & Raymond 1982). In addition to the Fe lines discussed above, the presence of nonresonance transitions due to

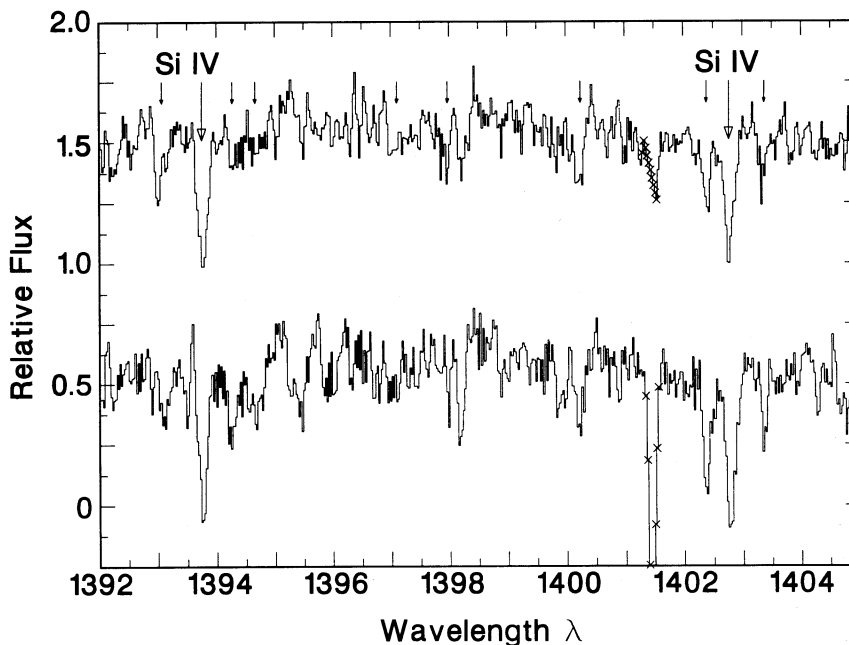


FIG. 6.—The same as Fig. 3, but showing the 1392–1404 Å region, which contains the Si IV doublet

N IV, O IV, and O V also argues strongly for a photospheric origin for the highly ionized features we have detected. The C IV, N V, and Si IV resonance lines are familiar features in the spectra of distant luminous stars, whose lines of sight pass through hot phases of the ISM (Jenkins 1987). However, such features have never, to our knowledge, been linked to any lines of sight within the local ISM ($d < 100$ pc). The Al III $\lambda 1854$ line is also a ground state transition and therefore could conceivably be of interstellar origin but its measured velocity in both of our stars is clearly that of the stellar photosphere. Moreover, its presence as an ISM feature would imply a relatively large column density which is not consistent with the observed strengths of other ISM lines and the absence of Si II $\lambda\lambda 1304$ and 1808 . We tentatively identify the Al III $\lambda 1854$ line as originating in the stellar photosphere; however, we note that due to the 28 eV ionization threshold of this ion, it is Al IV which should be the favored ionic state in the stellar atmosphere. We have searched for, but not found, any convincing features due to Al IV. This raises the possibility that the Al III may be of circumstellar origin. This will be discussed in more detail in the next section.

3.4. Unidentified Features

In addition to the host of features which have been identified in the echelle spectra of RE 2214–492 and RE 0623–377, there are also a number that are apparently real for which no identification is evident. Two can be seen near 1273 Å in the RE 2214–492 spectrum in Figure 5. Others present in both stars occur near 1227.51 Å, 1282.25 Å, 1501.78 Å, and 1579.70 Å. Checks of astronomical UV line lists such as Morton (1991) and Dean & Bruhweiler (1985) revealed no consistent identifications for these and a number of others. In addition, the detailed compilation of identified lines in laboratory spectra of Kelly (1987) was searched, with particular emphasis on other Fe group elements. There were coincidences within 0.1 Å with a number of ions, in particular Ni IV and Ni V, but the strong-

est predicted lines were notably absent. In view of the multiplicity of features from these ions that lie within the *IUE* SWP range, these coincidences are regarded as accidental. The line at 1579.70 Å does coincide with a Cr V line at 1579.696 Å, observed in sdO stars by Dean & Bruhweiler (1985). However, other more prominent lines of this same ion are not evident in our spectra.

3.5. Undetected Species: He II and O III

Of particular importance among the species not detected in RE 2214–492 and RE 0623–377 are He II and O III. We find no convincing evidence for the presence of an He II $\lambda 1640$ feature in either star, and we can place a conservative upper limit of 50 mÅ in both stars. Thus, neither star appears to be a DAO white dwarf. This absence of He II is also confirmed by the lack of the $\lambda 4686$ in the optical spectra of RE 2214–492 and RE 0623–377. Together these observations place an effective upper limit of $\log [N(\text{He})/N(\text{H})] < -4$, assuming a homogeneous composition or an H layer mass of $10^{-14} M_{\odot}$ for a stratified model, in these stars. We also find no evidence of O III in either star. This is significant, since O III has been reported in G191 B2B (Sion et al. 1992) and this ion may be responsible for the strong edges seen in the Wilkinson et al. (1992) EUV spectrum of G191 B2B. The significance of this lack of O III will be discussed in § 5. Finally, we have also searched for the presence of Fe VII. This ion has been reported in the spectra of the hot DAO stars NGC 7293 (Schönberner & Drilling 1985) and S216 (Tweedy & Napiwotzki 1992). Both these stars are H-rich PNs with effective temperatures near 100,000 K and $\log g \sim 7$ and are thus near the top of the white dwarf cooling sequence.

4. EXTREME ULTRAVIOLET AND X-RAY OBSERVATIONS

In addition to the survey observations of RE 2214–492 and RE 0623–377 with the S2, S1, and PSPC bands, pointed *ROSAT* data were also obtained (see Table 2). The main aim was to extend the survey coverage to longer wavelengths with the P1 filter of the WFC (150–220 Å), but this also gave us the

TABLE 5
OBSERVED *ROSAT* EUV AND X-RAY COUNT RATES AND UPPER LIMITS^a

INSTRUMENT/BAND	RE 2214–492	RE 0623–377	G191 B2B	FEIGE 24
	Observed constraints in counts s ⁻¹			
WFC P1	3.18 (0.07)	1.4 (0.01)	7.82 (0.03)	3.34 (0.02)
WFC S2	1.10 (0.03)	0.43 (0.02)	2.80 (0.04)	0.75 (0.03)
WFC S1	<0.016	<0.0064	0.063 (0.008)	0.0049 (0.0023)
PSPC survey	<0.013	<0.009	0.040 (0.022)	<0.014
PSPC pointed	<0.0028	<0.0024	N/A	N/A
<i>V</i> mag	11.4	12.2	11.73	12.56

^a 3 σ limits calculated using Bayesian statistics.

opportunity of obtaining PSPC exposures much deeper than available in the survey. Despite the increased exposure, neither star was detected by the PSPC. Table 5 summarizes the count rates and upper limits for these observations. All the WFC count rates have been corrected for known instrument sensitivity drifts so that they all correspond to the immediate post-launch calibration epoch to allow direct intercomparison (e.g., Willingale et al. 1993). The count rates for G191 B2B and Feige 24 are included in Table 5 for comparison.

It is possible to estimate the emergent flux for each star, facilitating comparison of the objects, by normalizing the count rate by the *V* magnitude and mean effective area of the instruments. We follow the prescription published in our earlier analysis of the *ROSAT* survey data (Barstow et al. 1993) listing the results in Table 6. In that earlier work we ignored the effect of interstellar opacity on the spectra since we were studying a variation in photospheric opacity spanning several orders of magnitude in flux. However, in this case we are looking at a group of stars with very similar properties where the interstellar absorption could affect the conclusions that we draw. The H I columns of G191 B2B and Feige 24 are relatively well determined, being $1.69 \times 10^{18} \text{ cm}^{-2}$ (Kimble et al. 1993) and $3.5 \times 10^{18} \text{ cm}^{-2}$ (Vennes 1992) respectively. At the moment we know little about the H I columns for RE 2214–492 and RE 0623–377. We do have a *Voyager* observation of RE 0623–377 which, from the absence of any emission shortward of the Lyman edge, gives us a lower limit to the column of $2.0 \times 10^{18} \text{ cm}^{-2}$. As we obtain similar heavy-element abundances for RE 2214–492 and RE 0623–377, the close agreement between the S2 fluxes suggests that both stars have similar H I densities. We can account for the effect of interstellar absorption by calculating the average attenuation for each bandpass using the known absorption cross sections

(e.g., Cruddace et al. 1974) and H I columns and then dividing the result into the flux estimates, as summarized in Table 6 (figures in brackets). These results serve to further emphasize the steeply cutoff nature of the EUV energy distributions of RE 2214–492 and RE 0623–377 with respect to G191 B2B and Feige 24.

5. DISCUSSION

From our combined observations of RE 2214–492 and RE 0623–377 it is clear that both objects are H-rich white dwarfs. The lack of any He $\lambda 1640$ feature in our *IUE* data and any evidence of He II $\lambda 4686$ in our optical data indicates that these stars are *not* DAO white dwarfs of high metal abundance, similar to Feige 55 (Bergeron et al. 1993) or S216 (Tweedy & Napiwotzki 1992). Rather, RE 2214–492 and RE 0623–377 are DA white dwarfs bearing a strong resemblance to G191 B2B and Feige 24, but are of higher temperature and higher heavy-element abundances. The temperatures of $T_{\text{eff}} = 63,500 \text{ K}$ and $T_{\text{eff}} = 60,300 \text{ K}$ which we find for RE 2214–492 and RE 0623–377, respectively, place these stars near the hot end of the DA sequence. For example, in study of the hottest DA stars present in the Palomar-Green (PG) survey (Green, Schmidt, & Liebert 1986), Holberg et al. (1989) found an effective upper limit of $T_{\text{eff}} = 70,000 \text{ K}$ for DA white dwarfs. Some hotter DA white dwarfs are known but they are central stars of PNs; well-studied examples include NGC 7293 and S216 (Tweedy & Napiwotzki 1992) with effective temperatures of 100,000 K and spectroscopic traces of He which classify them as DAO stars.

RE 2214–492 and RE 0623–377 are definitely not hot subdwarfs. Hot subdwarf stars such as BD +28°4211 or BD +75°325 (Dean & Bruhweiler 1985) exhibit many of the same echelle spectral features we have found in RE 2214–492 and

TABLE 6
NORMALIZED *ROSAT* EMERGENT EUV AND X-RAY FLUXES^a

INSTRUMENT/BAND	RE 2214–492	RE 0623–377	G191 B2B	FEIGE 24
	(Normalized count rates in count s ⁻¹)			
WFC P1	52.8 (52.8–330)	33.7 (85–210)	135 (314)	123 (615)
WFC S2	3.6 (3.6–7.4)	2.0 (2.9–4.2)	9.2 (12.8)	5.3 (10.2)
WFC S1	<0.026 (0.034)	<0.015 (0.020)	0.12 (0.14)	0.018 (0.023)
PSPC survey	<0.0007	<0.0006	0.0021	<0.0015
PSPC pointed	<0.0001	<0.0002		
H I column (cm ⁻²)	0–4 $\times 10^{18}$	2–4 $\times 10^{18}$	1.7 $\times 10^{18}$	3.5 $\times 10^{18}$

^a 3 σ limits calculated using Bayesian statistics.

TABLE 7
A COMPARISON OF ABUNDANCES AND ADOPTED EFFECTIVE TEMPERATURES

ELEMENT	ABUNDANCE Log $[N(X)/N(H)]$			
	G191 B2B	Feige 24	RE 2214–492	RE 0623–377
N	-5.59+0.14; -0.13	-5.11+0.38; -0.28	-4.44+0.08; -0.04	-4.64+0.06; -0.07
C	-5.74+0.02; -0.02	-6.26+0.04; -0.03	-5.74+0.03; -0.03	-6.08+0.03; -0.01
Si	-6.53+0.12; -0.13	-6.62+0.25; -0.23	-6.22+0.06; -0.15	-6.29+0.07; -0.07
$T_{\text{eff}}(K)$	58,000+2000; -2000	55,000+4000; -4000	63,500+2400; -1400	60,300+1700; -1300

RE 0623–377. However, such stars have much lower ($\log g \sim 4-5.5$) surface gravities than white dwarfs. The H I Lyman- α line and the Balmer lines from the optical data consistently place RE 2214–492 and RE 0623–377 in the surface gravity regime of white dwarfs, $\log g > 7.0$. A second strong argument against a subdwarf interpretation is the relatively strong EUV fluxes. With a few possible exceptions, hot subdwarf stars are not observed as EUV sources. For example, Sansom et al. (1992) searched the *ROSAT* bright source catalog for coincidences with known hot subdwarfs, finding only one coincidence involving a weak detection of a $V = 15.6$ sdO. In this same study none of the bright well-known subdwarfs were detected in either *ROSAT* band. Thus RE 2214–492 and RE 0623–377 appear to be true DA white dwarfs with effective temperatures in the range of the hottest members of this class with very high metal contents.

5.1. Comparisons with G191 B2B and Feige 24

The hot DA white dwarfs G191 B2B and Feige 24 are the two most natural objects with which to compare RE 2214–492 and RE 0623–377. Both G191 B2B and Feige 24 are among the hottest DA stars and have been the subject of numerous observations and studies. Moreover, there exist a substantial number of *IUE* echelle spectra of both stars. The co-addition of these spectra has allowed various investigators to conduct detailed and in-depth searches for weak features due to a number of important ions. In particular, Fe v has recently been detected in G191 B2B (Vennes et al. 1992; Sion et al. 1992; Tweedy 1991) and Feige 24 (Vennes 1992).

For the elements C, Si, and N it is possible to determine trace photospheric abundances for RE 2214–492 and RE 0623–377 from measurements of the equivalent widths of the C iv, Si iv, and N v feature and to directly compare abundances with those found in G191 B2B and Feige 24 for these elements. Using the results of Henry, Wesemael, & Shipman (1985), which compute the equivalent widths of various UV lines as a function of effective temperature and atomic abundance for DA white dwarf photospheres, we obtain the results given in Table 7. In obtaining these results we have used the observed equivalent widths of C iv $\lambda\lambda 1548, 1550$, Si iv $\lambda\lambda 1393, 1402$, and N v $\lambda\lambda 1238, 1242$. Sources for the equivalent width data are Table 3 of this paper for RE 2214–492 and RE 0623–377, Tweedy (1991) for G191 B2B, and Wesemael, Henry, & Shipman (1984) for Feige 24. Effective temperatures for G191 B2B and Feige 24 are adopted from the results of Kidder (1991) and Vennes (1992).

From the abundances in Table 7, G191 B2B and Feige 24 do not differ markedly in their C, Si, and N abundances. For RE 2214–492 and RE 0623–377, the N and Si abundances average about 0.5 dex higher than in G191 B2B and Feige 24, while the C abundances appear to be similar in all four stars. Direct comparisons, such as these, are not available for oxygen

since calculations similar to those of Henry et al. (1985) do not yet exist for O iv and O v.

One of us (G. V.) has calculated the expected equilibrium abundances of C, N, O, and Si in RE 2214–492 and RE 0623–377. These calculations are similar to those described in Vauclair (1989) and assume pure H model atmospheres having the T_{eff} and $\log g$ values we have determined for RE 2214–492 and RE 0623–377. Considering the abundances at a Rosseland mean optical depth of $\tau = 0.1$ to be representative of the abundances in each star, we provide equilibrium abundances in Table 8. These values should be compared with the observed values in Table 7. For N, the agreement between the predicted and the observed abundance is quite good. However, in the case of C and Si the observed abundances are considerably less, up to a factor of 40 less for C in RE 0623–377, than the expected equilibrium abundances. It is tempting to speculate that the lower than expected C and Si abundances could be attributed to the fact that the EUV fluxes available to levitate ions in these stars are substantially lower than those in the pure H model we have used. It would be necessary, however, to verify this by performing self-consistent equilibrium abundance calculations which incorporate Fe into the model atmosphere. The inability to predict reliably the observed abundance patterns in hot DA white dwarfs is not unique to RE 2214–492 and RE 0623–377. Vauclair (1989), Chayer et al. (1989), and Sion et al. (1992) all describe analogous problems with other DA white dwarfs.

The apparent lack of O iii in RE 2214–492 and RE 0623–377 is significant. As mentioned previously, strong edges, probably due to O iii, are seen in the EUV rocket spectrum of G191 B2B (Wilkinson et al. 1992), and absorption lines due to this ion are observed in the high S/N *HST* FOS spectrum of G191 B2B (Sion et al. 1992). The presence of considerable amounts of O iii in G191 B2B does not appear to be entirely consistent with the photospheric temperature. Recent work by Napiwotzki, discussed in Tweedy (1993), clearly indicates that O iv and O v, both of which are observed (Sion et al. 1992; Tweedy 1991), are the dominant ions in the photosphere of G191 B2B. The presence of significant O iii may indicate the existence of circumstellar material. If dense enough, it could contribute significantly to both the observed opacity at EUV

TABLE 8
CALCULATED EQUILIBRIUM ABUNDANCES

ELEMENT	ABUNDANCES Log $[N(X)/N(H)]$	
	RE 2214–492	RE 0623–377
N	-4.64	-4.54
C	-4.49	-4.44
Si	-5.52	-5.30
O	-4.80	-4.87

wavelengths and result in narrow interstellar-like lines in *IUE* echelle spectra. A similar situation may exist for Feige 24, where the evidence is more direct. Dupree & Raymond (1982) observed two sets of high-ionization lines in the *IUE* echelle spectra of this star. One set exhibited the orbital motion of the DA and another set corresponded to the system velocity of Feige 24. This latter material is presumed to be circumstellar material associated with the Feige 24 system. The origin of such material is unknown and could be associated with mass loss from the dMe secondary; alternatively it could be due to mass loss from the DA primary.

Although there exists no conclusive evidence of circumstellar material in the echelle spectra of RE 2214–492 and RE 0623–377, it is difficult to rule out such a possibility solely on the evidence of differing velocities among species. Taking for example RE 2214–492, the relatively low surface gravity of $\log 7.5$ implies a low mass and hence a low gravitational redshift. The 1σ upper limit on our spectroscopic gravity is 7.58. The largest gravitational redshift consistent with this gravity is for a zero temperature interior model, which yields a redshift of only $+14 \text{ km s}^{-1}$. Thus, circumstellar material kinematically at rest with respect to the photosphere could well blend with the stronger C IV, N V, and Si IV lines, resulting in a velocity centroid differing only slightly from the observed average velocity for all species. As discussed previously, it remains difficult to reconcile the presence of Al III, and the apparent lack of Al IV, with a photospheric origin and therefore this could indicate the presence of circumstellar material. The case for the existence of such circumstellar material would be improved if other lower ionization species could eventually be identified in higher S/N data.

Direct observational comparisons of RE 2214–492 and RE 0623–377 with G191 B2B and Feige 24, with respect to Fe content, are also of interest. First, as mentioned previously, RE 2214–492 and RE 0623–377 appear to be very similar stars from the perspective of their Fe content, with most of the apparent differences being attributed to the different S/N of the two spectra. Our observed Fe V line strengths can also be compared with those in G191 B2B, the only other hot DA white dwarf for which there is published equivalent width data on Fe (Sion et al. 1992; Tweedy 1991). Using four Fe V features which are common to Table 4 and the list of lines found by Tweedy (1991) in the high S/N spectra of G191 B2B ($\lambda\lambda 1402.4, 1440.5, 1456.2, \text{ and } 1469.0 \text{ \AA}$), we find an average strength of 47 mÅ for RE 2214–492 versus 25.8 mÅ for G191 B2B. Thus, the Fe V lines are not only more prevalent in RE 2214–492 and RE 0623–377 with respect to G191 B2B, they also appear to be stronger. No Fe V equivalent width measurements have been reported for Feige 24.

A detailed determination of the compositions of RE 2214–492 and RE 0623–377 requires an extensive set of self-consistent model atmosphere calculations with independently varying C, N, O, Si and Fe abundances to allow observed and predicted UV line profiles to be compared directly. Since this requires intensive computer processing over a substantial period of time we postpone this to a future paper. Nevertheless, we present a first estimate of the Fe abundances in these stars based on a subset of models where the C, N, O abundances are fixed and only the Fe is allowed to vary.

Synthetic spectra were computed using the self-consistent non-NLTE code of Werner (1986) incorporating the opacity sampling technique described by Dreizler & Werner (1993). In reporting this work, Dreizler & Werner (1993) note that the

inclusion of Fe line blanketing, at the levels we are concerned with here, does not appear to substantially affect the temperature structure of the atmosphere in the region where the UV lines are formed. However, it does have a substantial impact on the predicted continuum flux in the EUV. Therefore, the Fe abundances determined by Vennes et al. (1992) for G191 B2B and Feige 24, where Fe opacity was included in a pure H model without considering the effect on the model temperature and density structure, remain reasonable estimates with which we can compare our results. We can also argue that the impact on the atmospheric structure of C, N, O, and Si, which have many fewer EUV and UV lines than Fe, will be small and that fixing the abundances of these elements at some nominal value in our calculations will not lead to errors in our estimates of the Fe abundances.

Model calculations for RE 2214–492 and RE 0623–377 were performed at the specific temperatures and gravities determined from our optical data (e.g., $T_{\text{eff}} = 63,500 \text{ K}$, $\log g = 7.5$; $T_{\text{eff}} = 60,300 \text{ K}$, $\log g = 7.34$, respectively). In each case, the abundances relative to H were fixed at $C = 2.5 \times 10^{-6}$, $N = 3.2 \times 10^{-6}$, and $O = 8.4 \times 10^{-6}$. Si was not included. Models were calculated with varying Fe abundances of 1.0×10^{-5} , 3.0×10^{-5} , and 1.0×10^{-4} . These synthetic spectra were then compared visually with the *IUE* data to determine which Fe abundances best match the observations. This is illustrated in Figure 7 for RE 2214–491 and Figure 8 for RE 0623–377 which show the region of each *IUE* spectrum (1400–1480 Å) where the most prominent Fe V lines are found and models having Fe abundances of 3.0×10^{-5} and 1.0×10^{-4} . A remarkable agreement is found between the relative line strengths seen in both stars and those predicted. It is also apparent that the observed absolute line strengths lie in between the two models. From this we estimate that the abundance of Fe is $\log [N(\text{Fe})/N(\text{H})] = -4.25 \pm 0.25$. This value can be compared with the Fe abundances which Vennes et al. (1992) have estimated for G191 B2B and Feige 24 of $\log [N(\text{Fe})/N(\text{H})]$ to be -5.5 to -4.8 and -5.3 to -5.0 , respectively. Thus RE 2214–492 and RE 0623–377 are seen to have significantly higher Fe abundances than either Feige 24 or G191 B2B. However, it is worth noting that the observed Fe abundance levels for all four stars are clearly within the equilibrium abundance ranges predicted by Chayer et al. (1991) and Vennes et al. (1992) in their radiative levitation calculations for Fe in DA white dwarfs. It is interesting to note that we have folded the EUV energy distributions corresponding to the above models through the *ROSAT* filter responses and find, even with Fe abundances as large as 1.0×10^{-4} , that predicted count rates for both stars are one to two orders of magnitude too large. That is, the *ROSAT* observed fluxes in Table 5 clearly require a source of opacity in addition to those considered in our models. Work to identify the sources of this opacity is currently in progress.

The presence of Fe has been reported in several ionization stages in G191 B2B. Fe V is clearly the most prevalent ion, with numerous features reported by Sion et al. (1992), Tweedy (1991), and Vennes et al. (1992). Sion et al. (1992) report several tentative Fe VI lines blended with Fe V lines. However, from the lack of Fe VI features found in G191 B2B by Tweedy (1991) it is possible to infer a general upper limit of 15 mÅ for Fe VI line strengths in that star. Sion et al. (1992) also report possible blended features due to Fe III in the 1993–1997 Å region of their FOS spectrum. The existence of the Fe III ionization stage in the presence of the Fe V poses an apparent dilemma similar

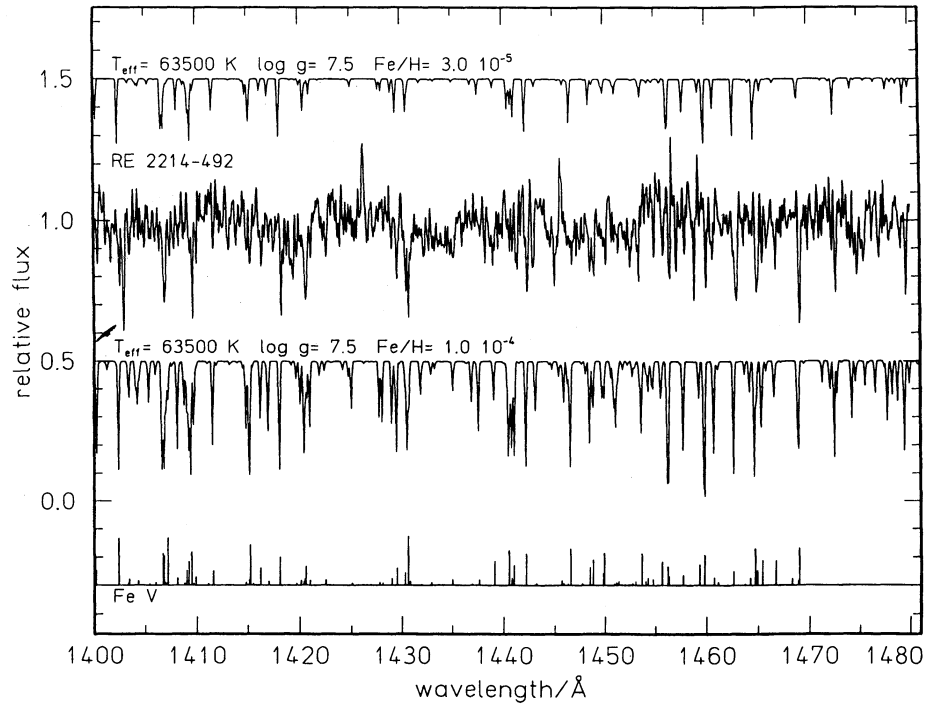


FIG. 7.—A comparison of the observed 1400–1480 Å spectrum of RE 2214–492 (normalized at 1.0) to model spectra containing Fe abundances of $N(\text{Fe})/N(\text{H}) = 3.0 \times 10^{-5}$ (above) and 1.0×10^{-4} (below). Both model spectra employ the temperature and gravity determined from the Balmer data. The line at the bottom labeled “Fe v” shows the locations and the line strengths (gf -values) used in the computation. We estimate the Fe abundance to lie between the two models shown here.

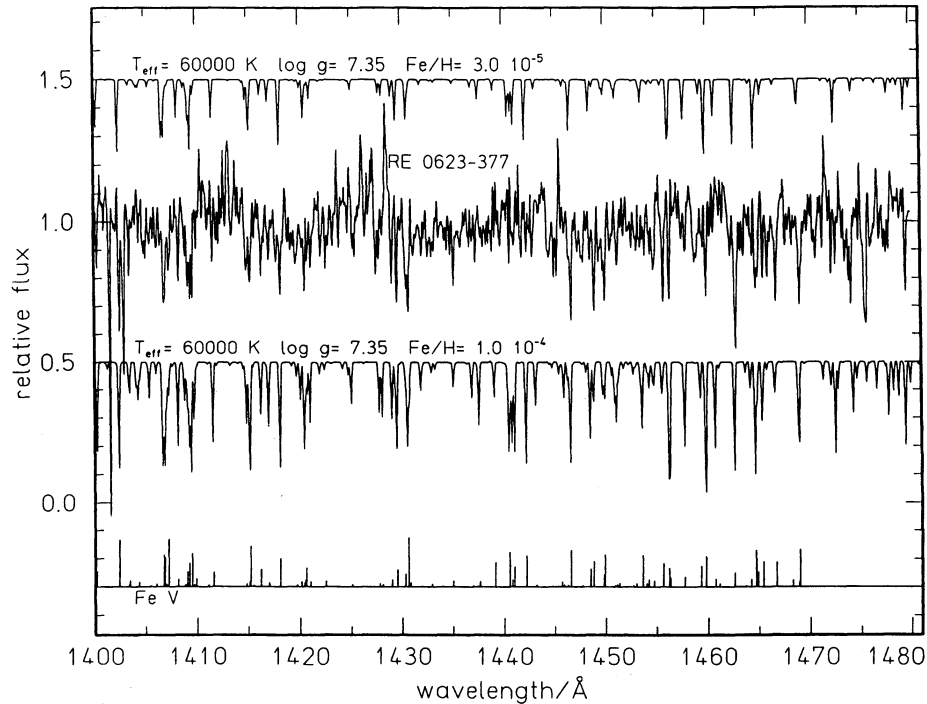


FIG. 8.—Same as for Fig. 7, except for RE 0623–377

to that of O III, discussed above. It is conceivable that the Fe III ions, if they exist, are also associated with circumstellar material.

The presence of Fe in a hot DA white dwarf, even at these trace levels, conceivably can produce significant effects well outside the EUV and soft X-ray bands. For example, both Dreizler & Werner (1992) and Vennes et al. (1992) have noted that the large number of transitions in the Fe IV, Fe V, and Fe VI ions, particularly in the EUV and UV bands, can alter the thermal structure of a DA atmosphere to the point that emergent flux predictions at longer wavelengths are significantly perturbed. Napiwotzki (1992) has recently demonstrated that H+He model atmospheres do not consistently fit the Balmer features in some hot DAO (H+He hybrid) white dwarfs. In one particular case, the central star of the planetary nebula S216, Tweedy & Napiwotzki (1992) have also identified numerous features due to Fe VI and Fe VII in *IUE* echelle observations of this hot ($\sim 100,000$ K) H-rich object. A similar situation appears to exist for Feige 55, a relatively bright hot DAO star, in which numerous Fe features are seen in *IUE* echelle spectra (Lamontagne et al. 1993). Bergeron et al. (1993) have analyzed the H I Balmer lines and the He II $\lambda 4686$ feature in Feige 55 and determined $T_{\text{eff}} = 60,340$ K, $\log g = 7.25$ and $\log [N(\text{He})/N(\text{H})] = -3.3$ for this star. They further demonstrated the ability to consistently model the observed Balmer features at these parameters, if they also include an photospheric Fe abundance of $\log [N(\text{Fe})/N(\text{H})] = -3.0$. This Fe abundance is approximately 20 times higher than we find for RE 2214–492 and RE 0623–377. It is uncertain whether such lower Fe abundances will result in detectable effects in the observed Balmer profiles of these two stars. However, we note that our present analyses of the Balmer profiles of these stars reveal no inherent inconsistencies between line profiles similar to those reported in some DAO stars.

Although the relationship of RE 2214–492 and RE 0623–377 to G191 B2B and Feige 24 is now well established, the evolutionary association of such stars to the rest of the white dwarfs sequence is less clear. For the hottest DA and DAO stars, metal abundances are seen to exhibit large variations. On one hand, there exist extreme metal-rich objects such as RE 2214–492, RE 0623–377, G191 B2B, and Feige 24 among the DA stars and Feige 55 among the DAO stars, while in the same temperature range are DA stars such as HZ 43 and DAO stars such as PG 1210–533 (see Holberg et al. 1988), which exhibit no apparent metals at all. For the hot DA stars, the *ROSAT* results of Barstow et al. (1993) clearly indicate that those having some metals predominate and that pure-HDA stars, such as HZ 43, are relatively rare. From this, one can conclude that it is not simple equilibrium abundances alone at a fixed T_{eff} and $\log g$ which determine the photospheric content of DA white dwarfs. Equilibrium abundances may thus represent the maximum potential abundance of a species but other factors may limit the amount of metals present in DA atmospheres. Gravity has been cited as a controlling factor. The main evidence for gravity has been the high gravity ($\log g \sim 8.5$) derived from the Lyman- α profile of HZ 43 (Holberg et al. 1986). It is now clear from Kidder (1991) and others that the Balmer profiles of HZ 43 yield a more conventional value of $\log g \sim 7.6$. Thus, a high gravity cannot explain the lack of metals in HZ 43. It is therefore likely that some aspect of white dwarf evolution which limits the equilibrium abundance of metals, such as the overlying H layer thickness, or alternately selective loss of metal ions during the early phases of white dwarf and pre-white dwarf evolution.

6. CONCLUSIONS

Among the DA white dwarfs detected in the *ROSAT* WFC all sky survey, RE 2214–492 and RE 0623–377 have the steepest observed short-wavelength cutoffs. Our *IUE* echelle observations of these two stars show them also to be the most metal-rich DA white dwarfs yet observed. Two previously known and well-studied metal-rich DA white dwarfs, G191 B2B and Feige 24, exhibit less extreme patterns of metal abundance and less steep EUV cutoffs. None of these stars shows any spectroscopic evidence for photospheric He. These results strongly suggest that the presence of heavy elements, not He, is responsible for the strong short-wavelength opacity seen in many of the hottest DA white dwarfs.

We find that each star exhibits a well-defined set of interstellar and photospheric features. The photospheric features are associated with C, N, O, Si, Al, and Fe and display a common characteristic velocity. The Fe transitions, which terminate in highly excited levels of Fe V and Fe VI, arise in the photospheres of these stars. The other metal features which share the same radial velocities with the Fe ions are also assumed to originate in the photospheres of these stars. The observed Fe abundances in RE 2214–492 and RE 0623–377 are $\log [N(\text{Fe})/N(\text{H})] = -4.25 \pm 0.25$, approximately 0.75 dex above the Fe abundances determined for G191 B2B and Feige 24, but far lower than the abundance inferred for the DAO star Feige 55. Previously published radiative levitation calculations indicate that the observed Fe abundance levels can be supported in the atmospheres of 60,000 K DA stars such as RE 2214–492 and RE 0623–377. However, similar calculations presented here for C and Si predict abundance levels for these elements significantly above those observed. Apart from the presence of Al III, we find no compelling evidence for circumstellar material associated with either star. In particular, there is no evidence of O III, which in G191 B2B may arise from circumstellar material. There is now strong evidence for the importance of trace heavy elements in the photospheres of hot DA white dwarfs. Since high abundances of Fe are associated with steep EUV cutoffs, it is likely that the two are directly connected, as has been suggested by Tweedy (1993).

The high abundances of heavy elements seen in RE 2214–492 and RE 0623–377 ensure these two stars will become key objects in the study of the radiative levitation of metals in DA photospheres, the nature of the soft X-ray opacity, and the early stages of the thermal and chemical evolution of white dwarfs in general. Of particular interest will be the development of fully self-consistent model atmospheres which include all of the species observed in RE 2214–492 and RE 0623–377. Such models should lead to considerably improved abundance estimates for all species as well as detailed EUV energy distributions.

An additional unique and important aspect of these two stars is their apparent brightness, which places them in the same category as G191 B2B. They are bright enough to be easily observed with a variety of instrumentation, and they will certainly be the subject of numerous follow-up observations over a wide range of wavelengths. Indeed, as more becomes known about these stars, they may, like other bright hot DA white dwarfs, serve as flux standards. Of particular interest will be short wavelength spectra of these stars from the EUVE. It is well within the capabilities of *IUE* to obtain additional echelle spectra of these stars which can be co-added with existing spectra to significantly enhance S/N. Similar co-added spectra have led to important new insights into the nature of G191

B2B and Feige 24. Existing ground-based observations are also currently limited and higher S/N spectra covering the Balmer region will be important.

We wish to acknowledge support from the following NASA grants: NAGW5-434 (J. B. H. and R. W. T.) and NAGW5-434

(E. M. S.). M. A. B. is funded through a SERC Advanced Fellowship, and M. C. M. by a SERC Studentship. We also wish to acknowledge the use of the grid of white dwarf model atmospheres computed by Detlev Koester and Tom Fleming for the upper limits from *ROSAT* PSPC Survey.

REFERENCES

- Barstow, M. A., et al. 1993, MNRAS, in press
 Bergeron, P., Wesemael, F., Lamontagne, R., & Chayer, P. 1993, ApJ, 407, L85
 Bruhweiler, F. C., & Feibelman, W. 1993, preprint
 Bruhweiler, F. C., & Kondo, Y. 1981, ApJ, 248, L123
 ———. 1983, ApJ, 269, 657
 Chayer, P., Fontaine, G., & Wesemael, F. 1989, in IAU Colloq. 114, White Dwarfs, ed. G. Wegner (Berlin: Springer) 253
 ———. 1991, in White Dwarfs, ed. G. Vauclair & E. Sion (Dordrecht: Kluwer), 249
 Cruddace, R., Paresce, F., Bowyer, S., & Lampton, M. 1974, ApJ, 187, 497
 Crutcher, R. M. 1982, ApJ, 254, 82
 Dean, C. A., & Bruhweiler, F. C. 1985, ApJS, 57, 133
 Dreizler, S., & Werner, K. 1992, in The Atmospheres of Early-Type Stars, ed. U. Heber & C. S. Jeffery (Berlin: Springer), 436
 ———. 1993, preprint
 Dupree, A. K., & Raymond, J. C. 1982, ApJ, 263, L63
 Ekberg, J. O. 1975a, Phys. Scripta, 11, 23
 ———. 1975b, Phys. Scripta, 12, 42
 Feibelman, W. A., & Bruhweiler, F. C. 1989, ApJ, 347, 901
 Green, R. F., Schmidt, M., & Liebert, J. 1986, ApJS, 61, 305
 Henry, R. B. C., Shipman, H. L., & Wesemael, F. 1985, ApJS, 57, 145
 Holberg, J. B., Kidder, K., Liebert, J., & Wesemael, F. 1989, in IAU Colloq. 114, White Dwarfs, ed. G. Wegner (Berlin: Springer), 188
 Holberg, J. B., Sion, E. M., Liebert, J., & Vauclair, G. 1988, in A Decade of UV Astronomy with *IUE* (ESA SP-281), Vol. 263
 Holberg, J. B., Wesemael, F., & Basile, J. 1986, ApJ, 306, 629
 Holberg, J. B., Wesemael, F., Wegner, G., & Bruhweiler, F. C. 1985, ApJ, 293, 294
 Jenkins, E. B. 1987, in Exploring the Universe with the *IUE* Satellite, ed. Y. Kondo (Dordrecht: Reidel), 531
 Jordan, S., & Koester, D. 1986, A&AS, 65, 367
 Jordan, S., Koester, D., Wulf-Mathies, C., & Brunner, H. 1987, A&A, 185, 253
 Kahn, S. M., Wesemael, F., Liebert, J., Raymond, J. C., Steiner, J. E., & Shipman, H. L. 1984, ApJ, 278, 255
 Kelly, R. L. 1987, J. Chem Phys. Ref. Data Suppl., 16, 1
 Kidder, K. 1991, Ph.D. thesis, Univ. Arizona
 Kimble, R., et al. 1993, ApJ, 404, 663
 Konigsberger, G. 1990, A&A, 235, 282
 Koester, D. 1989, ApJ, 342, 999
 ———. 1991, in IAU Symp. 145, Evolution of Stars: The Photospheric Abundance Connection, ed. G. Michaud & A. Tutakov (Dordrecht: Kluwer), 435
 Lallement, L., Bertaux, J.-L., & Clarke, J. C. 1993, Science, 260, 1095
 Lamontagne, R., Wesemael, F., Bergeron, P., Liebert, J., Fulbright, M. S., & Green, R. F. 1993, in White Dwarfs: Advances in Observations and Theory, ed. M. A. Barstow (NATO ASI Series), 437
 MacDonald, J. 1992, ApJ, 394, 619
 Mansperger, C. 1992, IUE Newsl., 49, 31
 Mason, K. O., et al. 1991, Vistas Astron., 34, 343
 Morton, D. C. 1991, ApJS, 77, 119
 Napiwotzki, R. 1992, in The Atmospheres of Early-Type Stars, ed. U. Huber & C. S. Jeffery (Berlin: Springer), 310
 Paerels, F. B. S., Bleeker, J. A. M., Brinkman, A. C., & Heise, J. 1986, ApJ, 309, L33
 Paerels, F. B. S., & Heise, J. 1989, ApJ, 339, 1000
 Petre, R., Shipman, H. L., & Canizares, C. R. 1986, ApJ, 304, 356
 Pounds, K. A., et al. 1993, MNRAS, 260, 77
 Sansom, A. E., Barstow, M. A., Holberg, J. B., & Kidder, K. M. 1992, MNRAS, 256, 1
 Schönberner, D., & Drilling, J. S. 1985, ApJ, 290, L49
 Shafer, R. A., Haberi, F., Arnaud, K. A., & Tennant, A. F. 1991, ESA TM-09
 Sion, E. M., Bohlin, R. C., Tweedy, R. W., & Vauclair, G. P. 1992, ApJ, 391, L29
 Sion, E. M., & Downes, R. A. 1992, ApJ, 396, L79
 Tweedy, R. W. 1991, Ph.D. thesis, Univ. Leicester
 ———. 1993, in White Dwarfs: Advances in Observations and Theory, ed. M. A. Barstow (NATO ASI Series), 317
 Tweedy, R. W., & Napiwotzki, R. 1992, MNRAS, 259, 315
 Vauclair, G. 1989, in IAU Colloq. 114, White Dwarfs, ed. G. Wegner (Berlin: Springer), 176
 Vennes, S. 1992, ApJ, 390, 601
 Vennes, S., Chayer, P., Fontaine, G., & Wesemael, F. 1989, ApJ, 336, L25
 Vennes, S., Pelletier, C., Fontaine, G., & Wesemael, F. 1988, ApJ, 331, 876
 Vennes, S., Chayer, P., Thronstensen, J. R., Bowyer, S., & Shipman, H. L. 1992, ApJ, 392, L27
 Vennes, S., Thejll, P., & Shipman, H. L. 1991, in White Dwarfs, ed. G. Vauclair & E. Sion (Dordrecht: Kluwer), 235
 Werner, K. 1986, A&A, 161, 177
 Wesemael, F., Henry, R. B. C., & Shipman, H. L. 1984, ApJ, 287, 868
 Wilkinson, E., Green, J. C., & Cash, W. 1992, ApJ, 397, L51
 Willingale, R., et al. 1993, in preparation